

**Korringa-like relaxation in the high-temperature phase of A-site ordered YBaMn<sub>2</sub>O<sub>6</sub>**

S. Schaile, H.-A. Krug von Nidda, J. Deisenhofer, and A. Loidl

*Experimentalphysik V, Center for Electronic Correlations and Magnetism, Institute for Physics,  
Augsburg University, D-86135 Augsburg, Germany*

T. Nakajima and Y. Ueda

*Material Design and Characterization Laboratory, Institute for Solid State Physics, University of Tokyo,  
5-1-5 Kashiwanoha, Kashiwa, Chiba 277-8581, Japan*

(Received 30 March 2012; published 11 May 2012)

We report on high-temperature electron spin resonance studies of A-site ordered YBaMn<sub>2</sub>O<sub>6</sub> and disordered Y<sub>0.5</sub>Ba<sub>0.5</sub>MnO<sub>3</sub>. In the disordered sample we find that the linewidth is governed by spin-spin relaxation processes as in many other manganite systems. In contrast we find a Korringa-like spin relaxation with a slope of about 1 Oe/K above the charge-ordering transition and extending up to 930 K in the metal ordered YBaMn<sub>2</sub>O<sub>6</sub> samples. A Korringa law is a clear feature of a truly metallic state, pointing to an unconventional high-temperature phase of these ordered manganites. In agreement with the electron spin resonance (ESR) intensity this suggests that in the metallic high-temperature phase the ESR signal stems from Mn<sup>4+</sup> core spins which relax via the quasidelocalized  $e_g$  electrons.

DOI: [10.1103/PhysRevB.85.205121](https://doi.org/10.1103/PhysRevB.85.205121)

PACS number(s): 76.30.-v, 75.47.Lx, 75.47.Gk, 71.30.+h

**I. INTRODUCTION**

During the last decades manganese-based oxides have been in the focus of condensed matter research due to their rich phenomenology ranging from colossal magnetoresistance effects to charge/orbital ordering and to multiferroicity. All of these aspects are predicted to occur in the phase space of half-doped manganites with chemical formula  $A_{0.5}A'_{0.5}MnO_3$  with A a trivalent rare-earth ion and  $A' = (Ca, Sr, Ba)$ . The role of disorder due to a random distribution of A and A' ions was found to be a decisive ingredient for this class of materials and, in particular, the possibility of growing both disordered  $A_{0.5}Ba_{0.5}MnO_3$  and ordered  $ABaMn_2O_6$  systems revealed significant differences in the corresponding phase diagrams.<sup>1-3</sup>

The A-site ordered manganites with perovskite structure contain two different ions (A and A'). These ions are arranged in two alternating AO and A'O layers which are stacked along the c axis, separated by MnO<sub>6</sub> octahedra. A-site order as high as 96% can be reached.<sup>4</sup> With exchanging the rare earth ions on the A site and Ba ions residing on the A' site a rich phase diagram can be obtained. With increasing ionic radius on the A site the system evolves from an orbital-ordered/charge-ordered, antiferromagnetic ground state to a ferromagnetic ground state for large ions.<sup>2</sup> The different valence of trivalent rare-earth ion and divalent Ba ion is leading to mixed valence on the Mn sites, resulting in a mixture of Mn<sup>3+</sup> and Mn<sup>4+</sup> ions. YBaMn<sub>2</sub>O<sub>6</sub>, with the largest discrepancy of the ionic radii between A and A' site, exhibits three peaks in the specific heat at 200 K ( $T_{c3}$ ), 480 K ( $T_{c2}$ ), and 520 K ( $T_{c1}$ ). Conductivity measurements show a metal-to-insulator transition at  $T_{c2}$ <sup>1</sup> and neutron-diffraction studies reveal a structural phase transition from monoclinic above  $T_{c1}$  to triclinic below.<sup>5</sup> The insulating phase below  $T_{c2}$  has been associated with charge and orbital order, accompanied by antiferromagnetic ordering below  $T_{c3}$ .<sup>6</sup> The two-step charge-ordering transition is accompanied by a strong change of the effective magnetic

moment from  $\mu_{\text{eff}} = 10.35\mu_B$  ( $=7.32\mu_B$  per Mn ion) below  $T_{c2}$  to  $\mu_{\text{eff}} = 6.22\mu_B$  ( $=4.40\mu_B$  per Mn ion) above  $T_{c1}$ . The susceptibility follows a Curie-Weiss law with  $\Theta = -512$  K below the charge-ordering transition and  $\Theta = 398$  K above. In contrast, the disordered system Y<sub>0.5</sub>Ba<sub>0.5</sub>MnO<sub>3</sub> does not show any charge and orbital ordering, but exhibits spin-glass-like features below 30 K.<sup>4</sup>

Electron spin resonance (ESR) provides a local probe to study the degrees of freedom of electron, spin, charge and orbitals, and their coupling to the lattice<sup>7-10</sup> which are considered to be the origin of the complex ordering phenomena in manganites. In our previous study on YBaMn<sub>2</sub>O<sub>6</sub> we reported ESR data up to a temperature of 600 K.<sup>11</sup> We show that the behavior of all ESR parameters in the low-temperature charge-ordered regime is strongly distinguished from that in the high-temperature metallic regime and with jump-like changes at  $T_{c1}$ . Focusing on the temperature dependence of the linewidth, the charge-ordered phase is strongly reminiscent of orbital-ordered La<sub>1-x</sub>Sr<sub>x</sub>MnO<sub>3</sub> ( $x < 0.15$ ), where the linewidth follows the temperature dependence of the orbital-order parameter.<sup>8,12,13</sup> In contrast, at high temperatures a quasilinear increase suggests a Korringa-type relaxation. However, due to the limited temperature range above  $T_{c1}$  a thermally activated behavior as reported for La<sub>1-x</sub>Ca<sub>x</sub>MnO<sub>3</sub><sup>14</sup> or a spin-spin relaxation dominated mechanism<sup>7</sup> could not be excluded, previously. In contrast to the static susceptibility the effective moment derived from the ESR intensity as  $\mu_{\text{ESR}} = 5.0(3)\mu_B$  ( $=3.53\mu_B$  per Mn ion) is within the expected range of the magnetic moment of Mn<sup>4+</sup> ions only, suggesting that the  $e_g$  electrons of the Mn<sup>3+</sup> do not contribute to the resonance absorption due to fast hopping between the Mn<sup>4+</sup> cores.<sup>11</sup>

Here we report on measurements up to 930 K, which unambiguously establish a Korringa-like increase and, hence, identify a truly metallic feature in this A-site ordered manganite. This behavior is contrasted with the results obtained for disordered Y<sub>0.5</sub>Ba<sub>0.5</sub>MnO<sub>3</sub>.

## II. EXPERIMENTAL DETAILS

Polycrystalline samples of the ordered system were prepared by solid-state reaction of  $R_2O_3$ ,  $BaCO_3$ , and  $MnO_2$  in Ar flow at 1573 K for 48 h. After sintering the oxygen deficiency in  $YBaMn_2O_{6-y}$  was about  $y \sim 0.9$ , but a final oxygen content of 6.00(2) could be realized by post-annealing at 773 K in pure oxygen for 48 h. Annealing at higher temperatures results in an exchange of  $A$ - and  $A'$ -site ions leading to disorder in the YO and BaO planes.<sup>4</sup> The ordering of the  $Y^{3+}$  and the  $Ba^{2+}$  cations was checked by powder x-ray diffraction (occupancy refinements) resulting in an ordering degree of nearly 100%. The disordered sample was prepared by the same starting materials and also showed full oxygen occupancy. Mixed powder was sintered at 1623 K in 1%  $O_2$ /Ar flow for 48 h and then heated at 1173 K in  $O_2$  flow for 48 h. The degree of disorder has been evaluated by Rietveld refinements similar to the procedure described in Ref. 4. Within experimental uncertainty of the powder XRD, no sizable impurities could be determined for both systems.

For ESR measurements in the temperature region  $300 < T < 1000$  K a Bruker Elexsys II spectrometer equipped with a Bruker ER 4114 HT X-Band ( $\nu = 9.49$  GHz) cavity was used. ESR detects the power  $P$  absorbed by the sample from the transverse magnetic microwave field as a function of the static magnetic field  $H$ . The signal-to-noise ratio of the spectra is improved by recording the derivative  $dP/dH$  using lock-in technique with field modulation. Due to large temperature gradients at high temperatures the sample temperature is corrected by calibration measurements at the actual sample site in the high-temperature cavity. To check the influence of different environmental conditions and temperature on the oxygen content of the samples at high temperatures, measurements have been performed in pure Ar at 0.7 bar pressure adjusted at room temperature and in air (open quartz tube).

## III. EXPERIMENTAL RESULTS AND DISCUSSION

Figure 1 shows ESR spectra of ordered  $YBaMn_2O_6$  for different temperatures in the paramagnetic regime. Even at elevated temperatures the signal is nicely detectable. The signal-to-noise ratio remains large up to highest temperatures, thus the absorption can be evaluated with high accuracy and can be described well by a single exchange narrowed Lorentzian line in the whole temperature range. Due to the large linewidth the resonance at  $-H_{res}$  has to be included.<sup>15</sup> In a usual metal one would expect a Dysonian line shape, but the degree of admixture of dispersion depends on the actual grain size and skin depth. The resistivity value reported for this polycrystalline material<sup>11</sup> is high compared to a good metal, leading to a skin depth larger than the grain size and a Lorentzian line shape.<sup>8</sup>

As expected for transition metals with less than half-filled  $d$  shells, the effective  $g$  factor remains constant in the metallic high-temperature regime at a value of  $g = 1.985$  (Fig. 2, lower frame) which within experimental uncertainty corresponds to the insulator single-ion value of  $Mn^{4+}$   $g = 1.994$  found in cubic symmetry.<sup>16</sup> Below  $T_{c1}$  the  $g$  factor slightly drops because of charge fluctuations and charge-ordering processes.

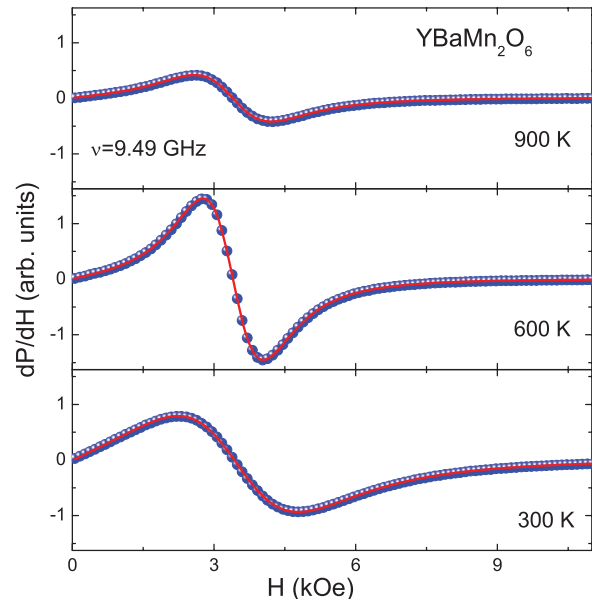


FIG. 1. (Color online) ESR spectra of  $YBaMn_2O_6$  at different temperatures below and above the charge-ordering transition ( $T_{c2} = 480$  K). The red line refers to the corresponding fit curves using Lorentzian line shapes (first derivative). The number of data points is reduced by a factor of 10.

The ESR intensity follows a Curie-Weiss law with  $\Theta = 387$  K in the high-temperature phase, indicating strong ferromagnetic correlations (Fig. 2, middle frame). Considering an uncertainty of about 20 K in  $\Theta$  due to uncertainties in the quality factor of

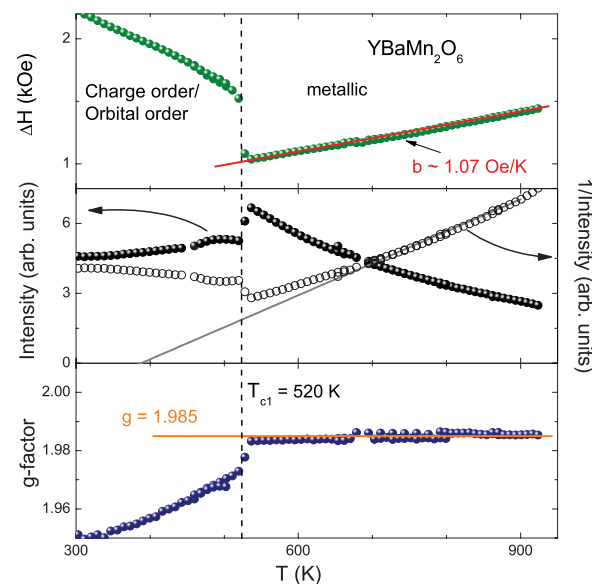


FIG. 2. (Color online) Upper frame: Temperature dependence of the ESR linewidth  $\Delta H$  in  $A$ -site ordered  $YBaMn_2O_6$ . A Korrington-type fit is indicated by a solid line. Middle frame: Temperature dependence of the ESR intensity and the inverse of the intensity. A Curie-Weiss fit is indicated by a solid line. Lower frame: Temperature dependence of the effective  $g$  factor. A constant  $g$  value  $g = 1.985$  is indicated by a solid line. The vertical dashed line is indicating the temperature of the charge-ordering transition ( $T_{c1} = 520$  K).

the cavity and sample temperature in the high-temperature region this value fits nicely to the values derived from susceptibility measurements.<sup>1</sup>

The temperature dependence of the ESR linewidth  $\Delta H$  from 300 to 930 K is shown in the upper frame of Fig. 2. As reported previously, in the low-temperature regime, between  $T_{c3} = 200$  K and  $T_{c1} = 520$  K, the ESR linewidth decreases from 3 to 1 kOe with increasing temperature.<sup>11</sup> Our new data reveal a sharp drop from 1.5 to 1 kOe at the structural phase transition at  $T_{c1} = 520$  K in agreement with a first-order transition. Above the structural transition at  $T_{c1} = 520$  K the linewidth increases with increasing temperature and shows a linear behavior which can be described by

$$\Delta H = \Delta H_0 + bT, \quad (1)$$

with a zero-temperature value  $\Delta H_0 = 420$  G and slope  $b = 1.07$  Oe/K. This value for the slope  $b$  differs by a factor of about 2 from the one obtained previously by fitting in a narrow temperature range above  $T_{c1}$ . This discrepancy stems from a temperature gradient between the sample's position inside the quartz tube and the position of the temperature probe. This gradient turned out to become significant above 500 K which is given as specification limit of the Bruker ER 4141VT System used previously. As mentioned above our new data has been obtained using an *in situ* calibration of the temperature at the sample position, thus ensuring a high accuracy of the actual sample temperature. All parameters coincided for heating and cooling.

To observe such a linear temperature dependence over a broad frequency range is rather uncommon for manganites, where the linewidth usually tends to saturate at high temperatures. This standard behavior is illustrated in Fig. 3 for the related disordered system  $Y_{0.5}Ba_{0.5}MnO_3$ . With increasing temperature the linewidth monotonously decreases approaching an asymptotic high-temperature value of about 1.5 kOe. At the same time the  $g$  factor is found to be temperature independent at  $g \approx 1.96$ . Note that this value is close to that of  $YBaMn_2O_6$  in the charge-ordered phase. The linewidth can be well described by the Kubo-Tomita approach for spin-spin relaxation in insulating paramagnets as applied in manganites

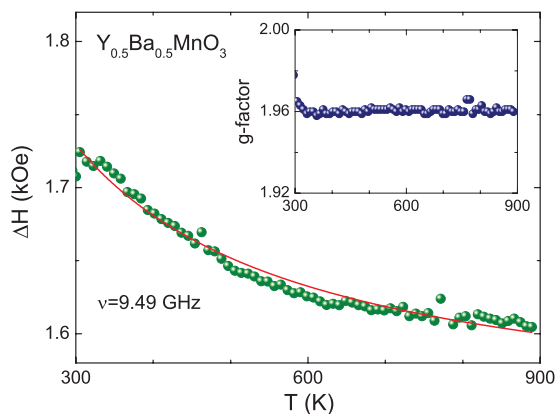


FIG. 3. (Color online) Temperature dependence of the ESR linewidth  $\Delta H$  in A-site disordered  $Y_{0.5}Ba_{0.5}MnO_3$  together with fit following Eq. (2). Inset: Temperature dependence of the effective  $g$  factor.

by Huber *et al.*<sup>7</sup>

$$\Delta H(T) = \frac{\chi_0(T)}{\chi_{dc}(T)} \Delta H_\infty = \frac{T - \Theta}{T} \Delta H_\infty, \quad (2)$$

where  $\chi_0(T)$  and  $\chi_{dc}(T)$  describe the susceptibilities of free and interacting spins, respectively, and  $\Delta H_\infty$  denotes the asymptotic high-temperature limit of the linewidth. The fit yields a Curie-Weiss temperature  $\Theta = -38$  K, in reasonable agreement with the susceptibility ( $\Theta = -18$  K determined from SQUID measurements), and  $\Delta H_\infty = 1.5$  kOe which is comparable to the values in many other manganite systems where the relaxation was found to be dominated by pure spin-spin relaxation processes.<sup>7,8,17</sup>

Three types of relaxation mechanisms are known to result in a strictly linear temperature dependence of the linewidth. The first corresponds to a modulation of the crystalline electric field by lattice vibrations, where only one phonon is involved in the relaxation process.<sup>16</sup> In the case of dilute magnetic ions in a nonmagnetic host lattice, this *direct spin-phonon process* yields a relaxation rate

$$\Delta H \propto \omega^n \coth\left(\frac{\hbar\omega}{2k_B T}\right), \quad (3)$$

with  $\omega$  being the resonance frequency, and  $n = 3$  or  $5$  corresponding to non-Kramers or Kramers ground states of the magnetic ions, respectively. In the limit  $k_B T \gg \hbar\omega$  the linewidth can be approximated by

$$\Delta H \propto \omega^{n-1} T. \quad (4)$$

The strong dependence on the resonance frequency or magnetic field is, however, not necessarily a characteristic property anymore in concentrated exchange-coupled magnetic systems.<sup>18</sup> A linear increase stemming from a direct phonon process was suggested for  $CrBr_3$ ,  $NiCl_2$  and other systems where the magnetic ion has no half-filled shell and spin  $S \geq 1$ .<sup>19,20</sup>

The second scenario was proposed by Seehra and Castner, where a linear temperature dependence of the linewidth can dominate the line broadening at temperatures of the order of the Debye temperature, if a large enough *static Dzyaloshinsky-Moriya interaction*  $\mathbf{D}(\mathbf{S}_i \times \mathbf{S}_j)$  between a pair of magnetic ions with spin  $S_i$  and  $S_j$  exists and is modulated by a single phonon for temperatures much higher than the Zeeman splitting  $k_B T \gg g\mu_B H$  and exchange coupling constants  $J \gg g\mu_B H$ <sup>18,21</sup>:

$$\Delta H \simeq \frac{4}{9} \frac{z}{g\mu_B} \frac{(\lambda R)^2 |\mathbf{D}|^2 J^2}{\rho \hbar^2} \left\langle \frac{1}{c_t^5} + \frac{2}{3} \frac{1}{c_l^5} \right\rangle k_B T. \quad (5)$$

Here  $z$  is the magnetic coordination number,  $\rho$  is the crystal density,  $c_{t,l}$  is the transverse and longitudinal sound velocity, and  $R$  is the nearest-neighbor distance. The parameter  $\lambda J \sim dJ/dr$  parametrizes the modulation of the exchange constant  $J$  by the ionic displacements due to the phonon and is a measure of the spin-phonon coupling.<sup>22-24</sup> Such a scenario has been proposed to be realized in the spin  $S = 1/2$  systems  $Cu(HCOO)_2 \cdot 4H_2O$ <sup>18</sup> and  $SrCu_2(BO_3)_2$ ,<sup>25</sup> but is usually overruled by the influence of the crystal electric field for systems with larger spins.

In early ESR studies in manganites the former *direct phonon process* had been evoked to describe the quasilinear behavior of the linewidth in some disordered manganites.<sup>26–28</sup> However, it was shown subsequently that a saturation behavior is reached at higher temperatures, which is characteristic of dominating spin-spin relaxation processes as described above for disordered  $\text{Y}_{0.5}\text{Ba}_{0.5}\text{MnO}_3$ .<sup>7</sup> Therefore, we discard the direct-phonon scenario for the high-temperature phase of  $\text{YBaMn}_2\text{O}_6$  and will concentrate on the third possibility to describe a linear temperature dependence, namely the well-known *Korringa-type relaxation*, which in contrast to the above mechanisms is governed by the presence of itinerant charge carriers in agreement with the metallic features of the high-temperature state, in particular the observation that the  $e_g$  electrons seem to act as quasidelocalized and do not participate in the resonant phenomenon as reported previously.<sup>11</sup>

The Korringa law for the linewidth is given by

$$\Delta H \propto (J_{\text{CE-ls}}^2(q))N^2(E_F)T, \quad (6)$$

where the slope is proportional to the square of the electronic density of states  $N(E_F)$  at the Fermi energy  $E_F$  and the exchange coupling  $J_{\text{CE-ls}}$  between the conduction electrons and the localized spins averaged over the momentum transfer  $q$  of the conduction electrons. The rather low value of  $b \simeq 1$  Oe/K might be indicative of a low density of state at the Fermi energy, but can also originate from the peculiarity of the manganite systems in terms of a bottlenecked relaxation as discussed below. The quantity  $\Delta H_0$  is affected by the relaxation times of ions and electrons, but is also strongly affected by crystal-field contributions, dipole-dipole interactions, or lattice defects.<sup>29</sup> It is known that these secondary effects<sup>30</sup> overlay the intrinsic contributions so strongly that a quantitative evaluation of this parameter is not possible. In contrast, the Korringa slope is robust with respect to secondary contributions.

Because of a lack of reports on Korringa-type relaxation in compounds containing  $\text{Mn}^{3+}$  or  $\text{Mn}^{4+}$  we have to compare the Korringa slope to  $\text{Mn}^{2+}$  systems with half-filled  $d$  orbitals. This scenario is closer to the situation of the half-filled  $t_{2g}$  orbitals in  $\text{Mn}^{4+}$  than to partially filled  $e_g$  orbitals in Jahn-Teller active  $\text{Mn}^{3+}$ . For  $\text{Mn}^{2+}$  a bottlenecked Korringa relaxation is the usual case, which is also of importance in manganese doped  $\text{La}_{2-x}\text{Sr}_x\text{CuO}_4$ .<sup>30</sup> This bottleneck can be opened by doping so that for example a Korringa slope of 45 Oe/K can be seen in unbottlenecked relaxation of highly diluted  $\text{Mn}^{2+}$  in  $\text{Ag:Mn:Ni}$ .<sup>31</sup> Other ESR results also support a bottlenecked spin relaxation in perovskite manganites.<sup>14,32</sup>

In the case of  $\text{YBaMn}_2\text{O}_6$  a strong bottleneck scenario seems applicable too. This bottleneck can be found in the relaxation of the conduction electrons to the phonon bath ( $B$ )  $\Gamma_{e_g \rightarrow B}$ , which is slower than the fast Overhauser relaxation  $\Gamma_{e_g \rightarrow \text{Mn}^{4+}}$  which supports a backscattering of the excitation from the conduction electrons to the  $\text{Mn}^{4+}$  spin before it can transfer its energy to the phonon bath. Thus the Korringa-slope is reduced by the ratio

$$\frac{\Gamma_{e_g \rightarrow B}}{\Gamma_{e_g \rightarrow \text{Mn}^{4+}} + \Gamma_{e_g \rightarrow B}}. \quad (7)$$

The relaxation path between  $\text{Mn}^{4+}$  spins and phonon bath is negligible because of weak  $S$ -state interactions, whereas

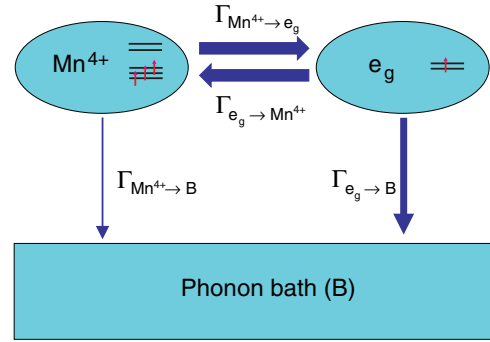


FIG. 4. (Color online) Schematic sketch of the bottleneck scenario for the spin relaxation of the local  $\text{Mn}^{4+}$  moments via the highly mobile  $e_g$  electron system in the metallic regime. The thickness of the arrows indicates the effectiveness of the relaxation paths.

the cross relaxation between  $\text{Mn}^{4+}$  spins and the conduction electrons is triggered by strong Hund's coupling and, thus, dominates the relaxation of the conduction electrons to the phonon bath even at highest temperatures. The linear temperature dependence of the linewidth is not affected, because the cross relaxation between  $\text{Mn}^{4+}$  spins and conduction electrons is temperature independent.<sup>29</sup> The relaxation of the conduction electrons to the phonon bath can be anticipated to be temperature independent as well, because the conductivity changes only weakly with temperature above  $T_{c1}$ .<sup>4</sup> The bottleneck scenario is further supported by the fact that we do not observe any significant shift of the  $g$  value which in contrary would be expected in the case of nonbottlenecked Korringa relaxation.

At present there does not seem to exist any microscopic model for mixed-valence manganites, which predicts a Korringa-like spin-relaxation rate as observed. However, Huber *et al.* suggested that mixed-valence manganites may be separated into a  $S = 3/2$  system originating from the  $\text{Mn}^{4+} t_{2g}$  core spins and a quasi-itinerant  $S = 1/2$  system corresponding to the  $e_g$  electrons,<sup>33</sup> which would support our bottleneck scenario (Fig. 4). Moreover, Moskvin proposed that the high-temperature, orbitally disordered state of  $\text{LaMnO}_3$  may be described by an electron-hole Bose liquid, which results from a charge-transfer instability leading to effective  $\text{Mn}^{2+}$ - $\text{Mn}^{4+}$  configurations and metallic-like behavior.<sup>34</sup> Similarly, such a mechanism may be realized in our system above the charge- and orbital-ordering transition. One may speculate that the Korringa-like behavior of the ESR linewidth could be a signature of such a charge-disproportion picture and we hope that our results will foster further theoretical efforts with regard to spin relaxation in manganites.

#### IV. CONCLUSIONS

In summary, we investigated the high-temperature ESR behavior in polycrystalline samples of ordered  $\text{YBaMn}_2\text{O}_6$  and disordered  $\text{Y}_{0.5}\text{Ba}_{0.5}\text{MnO}_3$ . The latter exhibits a conventional temperature dependence of the linewidth due to spin-spin relaxation. The linear high-temperature increase of the linewidth over a temperature range of 400 K is a unique feature for  $A$ -site ordered  $\text{YBaMn}_2\text{O}_6$ . It can be well described by a bottlenecked Korringa relaxation and indicates a scenario where highly

mobile  $e_g$  electrons are present on a  $Mn^{4+}$  background. This is in accordance to the observed magnetic moment for  $Mn^{4+}$  only, obtained from the ESR intensity. The low  $g$  shift matches the nearly quenched orbital moment of the half-filled  $t_{2g}$  shell of this  $Mn^{4+}$  background as well as the bottleneck scenario. To further analyze this mechanism single crystal measurements should be performed to enhance the accuracy of conductivity measurements at high temperatures and give an insight into a possible anisotropy of the spin relaxation.

## ACKNOWLEDGMENTS

It is a pleasure to thank D. L. Huber, M. V. Eremin, A. S. Moskvin, and N. Pascher for fruitful discussions. We are grateful to Dana Vieweg for susceptibility measurements. This work is partially supported by the Deutsche Forschungsgemeinschaft via the Collaborative Research Center TRR 80 (Augsburg-Munich).

- 
- <sup>1</sup>T. Nakajima, H. Kageyama, and Y. Ueda, *J. Phys. Chem. Solids* **63**, 913 (2002).
- <sup>2</sup>D. Akahoshi, M. Uchida, Y. Tomioka, T. Arima, Y. Matsui, and Y. Tokura, *Phys. Rev. Lett.* **90**, 177203 (2003).
- <sup>3</sup>T. Nakajima and Y. Ueda, *J. Appl. Phys.* **98**, 046108 (2005).
- <sup>4</sup>T. Nakajima, H. Yoshizawa, and Y. Ueda, *J. Phys. Chem. Solids* **73**, 2283 (2004).
- <sup>5</sup>A. J. Williams and J. P. Attfield, *Phys. Rev. B* **72**, 024436 (2005).
- <sup>6</sup>A. Daoud-Aladine, C. Perca, L. Pinsard-Gaudart, and J. Rodríguez-Carvajal, *Phys. Rev. Lett.* **101**, 166404 (2008).
- <sup>7</sup>D. L. Huber, G. Alejandro, A. Caneiro, M. T. Causa, F. Prado, M. Tovar, and S. B. Oseroff, *Phys. Rev. B* **60**, 12155 (1999).
- <sup>8</sup>V. A. Ivanshin, J. Deisenhofer, H.-A. Krug von Nidda, A. Loidl, A. A. Mukhin, A. M. Balbashov, and M. V. Eremin, *Phys. Rev. B* **61**, 6213 (2000).
- <sup>9</sup>B. I. Kochelaev, E. Shilova, J. Deisenhofer, H.-A. Krug von Nidda, A. Loidl, A. A. Mukhin, and A. M. Balbashov, *Mod. Phys. Lett. B* **17**, 459 (2003).
- <sup>10</sup>J. Deisenhofer, D. Braak, H.-A. Krug von Nidda, J. Hemberger, R. M. Eremina, V. A. Ivanshin, A. M. Balbashov, G. Jug, A. Loidl, T. Kimura, and Y. Tokura, *Phys. Rev. Lett.* **95**, 257202 (2005).
- <sup>11</sup>D. Zakharov, J. Deisenhofer, H.-A. Krug von Nidda, A. Loidl, T. Nakajima, and Y. Ueda, *Phys. Rev. B* **78**, 235105 (2008).
- <sup>12</sup>J. Deisenhofer, B. I. Kochelaev, E. Shilova, A. M. Balbashov, A. Loidl, and H.-A. Krug von Nidda, *Phys. Rev. B* **68**, 214427 (2003).
- <sup>13</sup>G. Alejandro, M. C. G. Passeggi, D. Vega, C. A. Ramos, M. T. Causa, M. Tovar, and R. Senis, *Phys. Rev. B* **68**, 214429 (2003).
- <sup>14</sup>D. J. Twitchen, J. M. Baker, M. E. Newton, and K. Johnston, *Phys. Rev. B* **61**, 9 (2000).
- <sup>15</sup>J. P. Joshi and S. V. Bhat, *J. Magn. Reson.* **168**, 284 (2004).
- <sup>16</sup>A. Abragam and B. Bleaney, *EPR in Transition Metal Ions* (Dover, New York, 1970).
- <sup>17</sup>J. Deisenhofer, M. Paraskevopoulos, H.-A. Krug von Nidda, and A. Loidl, *Phys. Rev. B* **66**, 054414 (2002).
- <sup>18</sup>M. S. Seehra and T. C. Castner, *Phys. Kondens. Mater.* **7**, 185 (1968).
- <sup>19</sup>R. J. Birgeneau, L. W. Rupp Jr., H. J. Guggenheim, P. A. Lindgard, and D. L. Huber, *Phys. Rev. Lett.* **30**, 1252 (1973).
- <sup>20</sup>D. L. Huber and M. S. Seehra, *J. Phys. Chem.* **36**, 723 (1975).
- <sup>21</sup>T. G. Castner Jr. and M. S. Seehra, *Phys. Rev. B* **4**, 38 (1971).
- <sup>22</sup>W. Baltensperger and J. S. Helman, *Helv. Phys. Acta* **41**, 668 (1968).
- <sup>23</sup>Ch. Kant, J. Deisenhofer, T. Rudolf, F. Mayr, F. Schrettle, A. Loidl, V. Gnezdilov, D. Wulferding, P. Lemmens, and V. Tsurkan, *Phys. Rev. B* **80**, 214417 (2009).
- <sup>24</sup>Ch. Kant, M. Schmidt, Z. Wang, F. Mayr, V. Tsurkan, J. Deisenhofer, and A. Loidl, *Phys. Rev. Lett.* **108**, 177203 (2012).
- <sup>25</sup>A. Zorko, D. Arcon, H. van Tol, L. C. Brunel, and H. Kageyama, *Phys. Rev. B* **69**, 174420 (2004).
- <sup>26</sup>M. S. Seehra, M. Ibrahim, V. S. Babu, and G. Srinivasan, *J. Phys.: Condens. Matter* **8**, 11283 (1996).
- <sup>27</sup>S. E. Lofland, P. Kim, P. Dahiroc, S. M. Bhagat, S. D. Tyagi, S. G. Karabashev, D. A. Shulyatev, A. A. Arsenov, and Y. Mukovskii, *Phys. Lett. A* **233**, 476 (1997).
- <sup>28</sup>C. Rettori, D. Rao, J. Singley, D. Kidwell, S. B. Oseroff, M. T. Causa, J. J. Neumeier, K. J. McClellan, S.-W. Cheong, and S. Schultz, *Phys. Rev. B* **55**, 3083 (1997).
- <sup>29</sup>S. E. Barnes, *Adv. Phys.* **30**, 801 (1981).
- <sup>30</sup>B. I. Kochelaev, L. Kan, B. Elschner, and S. Elschner, *Phys. Rev. B* **49**, 13106 (1994).
- <sup>31</sup>B. Elschner and A. Loidl, in *Handbook on the Physics and Chemistry of Rare Earths*, edited by K. A. Gschneidner Jr. and L. Eyring, Vol. 24 (Elsevier, Amsterdam, 1997), p. 221.
- <sup>32</sup>B. Padmanabhan, A. Sharma, S. S. Rao, S. Elizabeth, H. L. Bhat, and S. V. Bhat, *Physica B* **398**, 107 (2007).
- <sup>33</sup>L. Huber, D. Laura-Ccahuana, M. Tovar, and M. T. Causa, *J. Magn. Mater.* **310**, 604 (2007).
- <sup>34</sup>A. S. Moskvin, *Phys. Rev. B* **79**, 115102 (2009).